Western Canada detailing for reinforcing bar connections of hollow-core slabs to masonry walls: Tension tests

Yazan Al-Hatamleh, Yasser M. Selmy, Karl Truderung, and Ehab F. El-Salakawy

- Focused on practices in western Canada, this study investigates the performance of hollow-core-slab–to–masonry wall connections under tensile loads and assesses their reliability in multistory applications.
- Six full-scale specimens were constructed and tested under monotonic tensile loading to examine the effects of reinforcing bar shape, placement, and simulated vertical position within a ten-story structure.
- Tests were conducted under controlled laboratory conditions to simulate connections replicating construction-level detailing and axial loading.

Precast, prestressed hollow-core slabs have become an integral part of modern construction, offering significant advantages over traditional solid concrete slabs. Hollow-core slabs are characterized by continuous hollow sections running along their lengths, which significantly reduce their self-weight while optimizing material usage. Despite their reduced weight, hollow-core slabs exhibit exceptional strength due to the use of prestressing, where high-strength steel tendons are pretensioned to reduce deflection and cracking. This combination of reduced weight and prestressing allows hollow-core slabs to cover longer spans than conventional concrete slabs, making them ideal for applications requiring long spans, such as parking structures, high-rise buildings, and industrial structures.

In structural applications, hollow-core slab segments are installed side by side and supported by structural elements such as steel beams, masonry walls, or precast concrete beams and walls. Maintaining a reliable load path between the hollow-core slab diaphragm and its supports is essential for floor-system integrity, particularly in multistory buildings and under wind, seismic, or other accidental lateral loads. Grouted shear keys interconnect the slabs, providing transverse stability and enabling the assembly to function as a continuous horizontal diaphragm. Reinforcing bars, known as structural integrity ties, embedded within the shear keys or edge hollow-cores, transfer lateral forces to the supporting elements. Inadequate or improperly detailed connections can compromise diaphragm action, potentially leading to interelement sliding or structural failure.

Consequently, North American standards specify minimum tensile demands for integrity ties to ensure floor-system continuity. Canadian Standards Association (CSA) Group's *Design of Concrete Structures* (CSA A23.3:24)[1] and the American Concrete Institute's (ACI's) *Building Code for Structural Concrete—Code Requirements and Commentary* (ACI CODE-318-25)[2] prescribe minimum tensile strength requirements for structural integrity ties. These requirements are primarily intended to resist axial forces that could pull the hollow-core slab units away from their supports, thereby preserving overall floor system integrity during abnormal loading events. For single-story structures, CSA A23.3:24 specifies a minimum factored tensile resistance of 5.0 kN/m (0.34 kip/ft), which represents a line load per unit length of slab support, essentially ensuring that along every meter of floor width, sufficient tie capacity exists to prevent separation during lateral or vertical displacements. In contrast, ACI 318-25 requires a slightly lower nominal tensile capacity of 4.4 kN/m (0.30 kip/ft). For structures of two stories or more, CSA A23.3:24 requires a factored tensile resistance of 14 kN/m (0.96 kip/ft), whereas ACI sets a higher nominal threshold of 22 kN/m (1.50 kip/ft) for structures of three stories or taller.

Despite these code provisions for minimum tensile strength, neither CSA nor ACI provides explicit guidance on the response of hollow-core-slab–to–support connections under various in-plane loading conditions. In-plane tension (pull-away, perpendicular to the support), compression (push-in, perpendicular to the support), and shear (sliding, parallel to the support) may occur due to reversible lateral loading. The connection response depends on interface shear transfer, clamping (gravity and axial compression), bar geometry, and the detailing of bar anchorage into the wall and slab. Thus, understanding the full in-plane behavior is essential, particularly in seismic or high-wind regions, where such forces may act simultaneously or cyclically.

The hollow-core-slab–to–support bar connections are categorized as either end-bearing connections, where slab voids are perpendicular to the support, or side connections, where voids are parallel to the support (**Fig. 1**). Detailing practices for hollow-core-slab–to–masonry wall bar connections vary regionally across Canada. In western Canada, 10M (no. 3) Grade 400W (58 ksi) connection bars are typically embedded in the hollow-core slab grout key or edge pocket and anchored

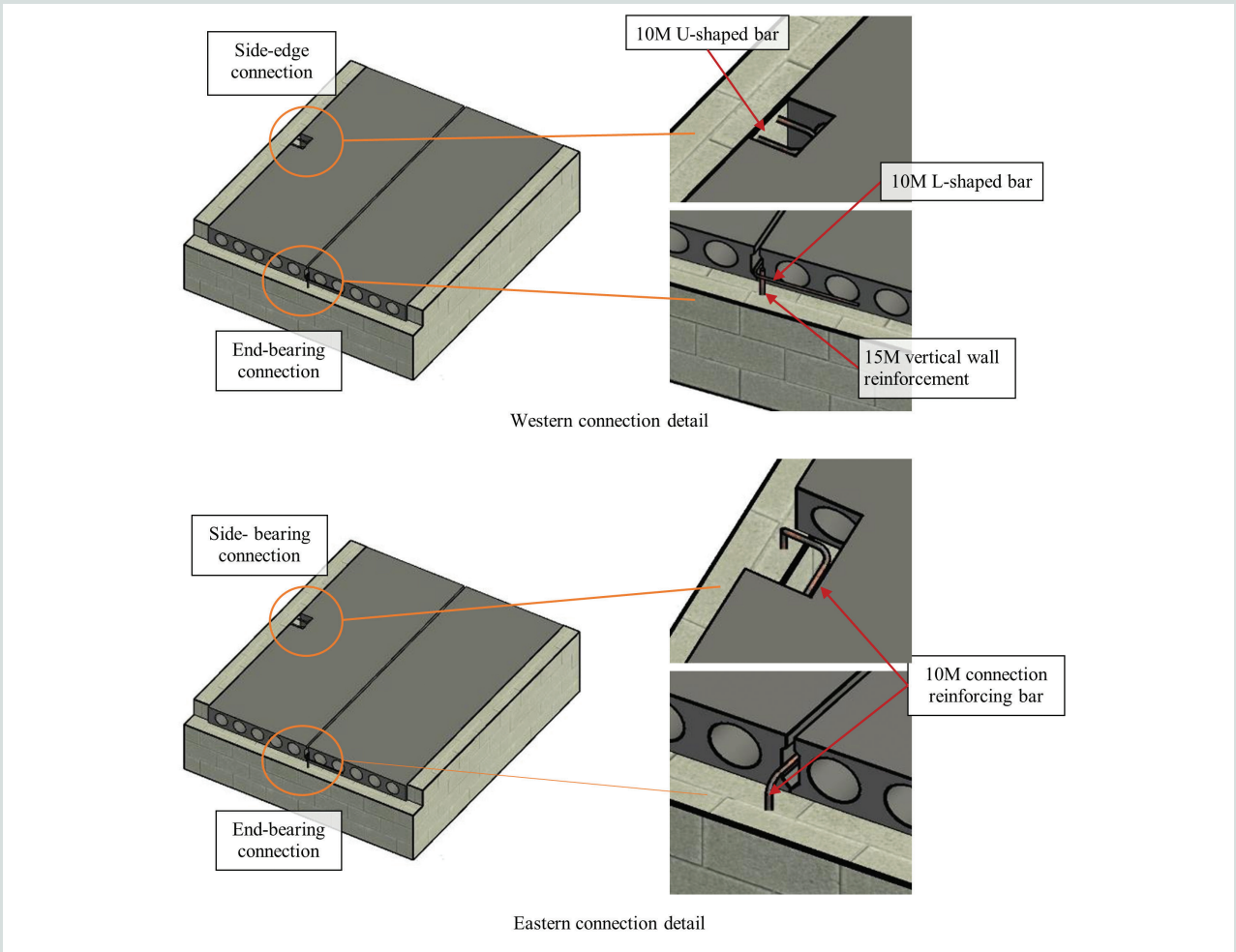

Figure 1. Canadian end- and side-connection details before grouting. Note: 10M = no. 3; 15M = no. 5.

into the masonry wall by engaging vertical reinforcement, usually 15M (no. 5) Grade 400W bars. The connection bars are either L shaped or U shaped. The L-shaped configuration wraps around the vertical wall reinforcement and extends into the hollow-core slab shear key (Fig. 1), while the U-shaped configuration inserts both legs into a preslotted hollow-core slab void and wraps behind the vertical wall reinforcement before being grouted in place. For side-edge connections, U-shaped bars are inserted through slab pockets and anchored into masonry blocks via predrilled holes (Fig. 1).

In eastern Canada, connections typically omit vertical wall reinforcement. Instead, a 10M (no. 3) L-shaped reinforcing bar is embedded in the hollow-core slab grout key or edge pocket and extends downward into a predrilled, snug-fit dry hole in the masonry wall. This L-shaped bar is either left unbonded or secured using epoxy within the wall (Fig. 1).

The end-bearing integrity ties are placed between hollow-core slab segments and spaced at 1220 mm (48 in.). For side-edge connections, the ties are spaced at a maximum of 3000 mm (118 in.). Proper anchorage of the integrity ties to the hollow-core slabs is crucial, requiring a minimum embedment length of 450 mm (17.7 in.) inside the grouted joints for a secure connection.[3]

Research on the performance of bar connections of hollow-core slab to masonry under various in-plane loads, such as tension, compression, and shear, remain limited. Hernandez Brito et al.[3] examined eastern Canada detailing of hollow-core-slab–to–masonry walls, reporting that connections subjected to compression failed with bar yielding followed by masonry crushing. Tensile forces led to masonry block face spalling and large displacement, reducing hollow-core slab bearing. Connections under shear forces exhibited failure by bar bending and pullout; however, using adhesives improved load transfer and prevented pullout. The study further concluded that aligning connection bars with the hollow-core slab horizontal plane improved lateral resistance and reduced displacement. While the investigated connections met code requirements for one- and two-story buildings, they were found to be inadequate for structures of three stories or taller, where higher-integrity tie forces govern the design requirements.

These findings underscore the need to evaluate western Canada detailing, particularly under axial loads from upper stories and other vertical forces, to ensure robust performance in multistory contexts. Such analysis is vital for developing resilient hollow-core slab designs that withstand diverse loading scenarios.

Research significance

The growing use of precast concrete systems in Canada, particularly those integrating hollow-core slab with masonry walls, underscores the need for a comprehensive evaluation of hollow-core-slab–to–masonry wall connections. This study investigates the performance of these connections under tensile loads, detailed per western Canada practices, to assess their reliability in multistory applications. The findings aim to inform the development of robust design methodologies enhancing safety and construction efficiency in multistory buildings that combine hollow-core slab and masonry walls. Moreover, this research addresses deficiencies in current North American design codes, providing evidence-based insights to support updates to standards and bridge existing knowledge gaps.

Experimental program

Test specimens

This study is part of a comprehensive research program at the University of Manitoba investigating the behavior of hollow-core slab bar connections to various supporting elements, including steel beams, precast concrete members, and masonry walls. The present phase focuses on end-bearing hollow-core-slab–to–masonry wall connections detailed according to western Canada practices. A total of six full-scale specimens were constructed and tested under monotonic tensile (pull-away) loading to examine the effects of reinforcing bar shape, placement, and simulated vertical position within a ten-story structure.

Four of the specimens used L-shaped bars to connect two adjacent hollow-core-slab units to the masonry wall, while the remaining two incorporated U-shaped bars connecting a single hollow-core-slab unit. The L-bar specimens simulated connections at four building levels: the roof, a parapet condition (roof level with additional masonry above), the fifth floor, and the first floor. In a ten-story structure, the U-bar specimens represented the roof and parapet conditions. In the L-bar specimens, the reinforcing bar was looped around the vertical wall reinforcement and grouted into the shear key between the two slabs, extending into slab A and oriented parallel to the wall axis (**Fig. 2**). In the U-bar specimens, a 102 mm (4 in.) slot was precut into one of the hollow-core-slab cores to accommodate the bar legs. The remaining 114 mm (4.5 in.) of wall thickness, along with any interior voids, was filled with grout to the height of the slab. Void plugs were inserted into the core to manage grout flow and ensure proper consolidation (Fig. 2).

Details of specimens, including bar configuration, number of slabs, and simulated floor level, are summarized in **Table 1**. In L-bar specimens, slab A refers to the hollow-core slab toward which the bar is bent; slab B is the adjacent unit (Fig. 2). Specimen identification followed a four-part designation:

- EB denotes end-bearing configuration.
- T denotes tension loading.
- L or U represents the bar shape.
- Floor level is shown as R for roof, P for parapet, 5 for fifth floor, and 1 for first floor.

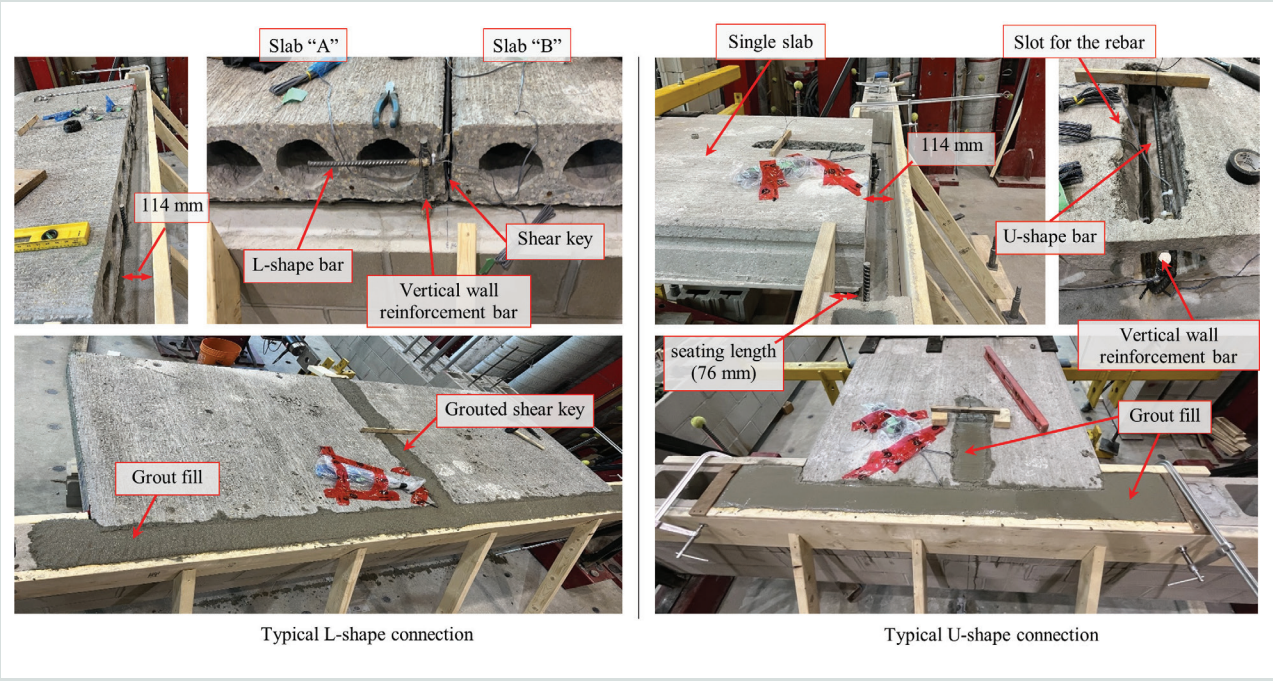

Figure 2. Details of test specimens EB-T-L-R (end bearing configuration with tensile loading and an L-shaped bar connection at the roof level) and EB-T-U-R (end bearing configuration with tensile loading and a U-shaped bar connection at the roof level). Note: 1 mm = 0.0394 in.

Table 1. Details of test specimens

Specimen ID	Bar shape	Represented floor in ten-story building	Number of segments
EB-T-L-R	L	Roof level	2
EB-T-L-P	L	Tenth floor (under parapet wall weight only)	2
EB-T-L-5	L	Fifth floor (under weight of five floors)	2
EB-T-L-1	L	First floor (under weight of nine floors)	2
EB-T-U-R	U	Roof level	1
EB-T-U-P	U	Tenth floor (under parapet wall weight only)	1

Note: EB-T-L-P = end bearing configuration with tensile loading and an L-shaped bar connection with a parapet configuration; EB-T-L-R = end bearing configuration with tensile loading and an L-shaped bar connection at the roof level; EB-T-L-1 = end bearing configuration with tensile loading and an L-shaped bar connection at the first story; EB-T-L-5 = end bearing configuration with tensile loading and an L-shaped bar connection at the fifth story; EB-T-U-P = end bearing configuration with tensile loading and a U-shaped bar connection with a parapet configuration; EB-T-U-R = end bearing configuration with tensile loading and a U-shaped bar connection at the roof level.

Each hollow-core slab segment measured 1220 × 1220 mm (48 × 48 in.) in plan and 203 mm (8 in.) in thickness and was seated on the masonry wall with a bearing length of 76 mm (3 in.), exceeding the minimum requirement of 50 mm (2 in.) specified by CSA A23.3:24[1] and the *CPCI Design Manual: Precast and Prestressed Concrete*.[4] Bearing was provided using Korolath bearing strips (3 × 50 × 1220 mm [0.12 × 2 × 48 in.]) beneath each unit to ensure uniform load distribution, installed inset from unarmored slab edges to maintain a minimum clear distance of 25 mm (1 in.), thereby satisfying the edge-distance requirements of ACI 318-25[2] for bearing pads.

The masonry walls were constructed by professional masons to reflect standard construction quality and consisted of single-wythe assemblies measuring 190 mm (7.5 in.) in thickness and 3990 mm (157 in.) in length. Wall height varied according to the simulated floor level: roof-level specimens included four masonry courses, while intermediate-level specimens included an additional three courses above the slab for a total of seven. The walls were built using 190 × 190 × 390 mm (7.5 × 7.5 × 15.3 in.) concrete masonry units (CMUs), including plain end units at course ends, two-cell stretcher blocks in unreinforced courses, and knockout web bond blocks in reinforced courses (**Fig. 3**).

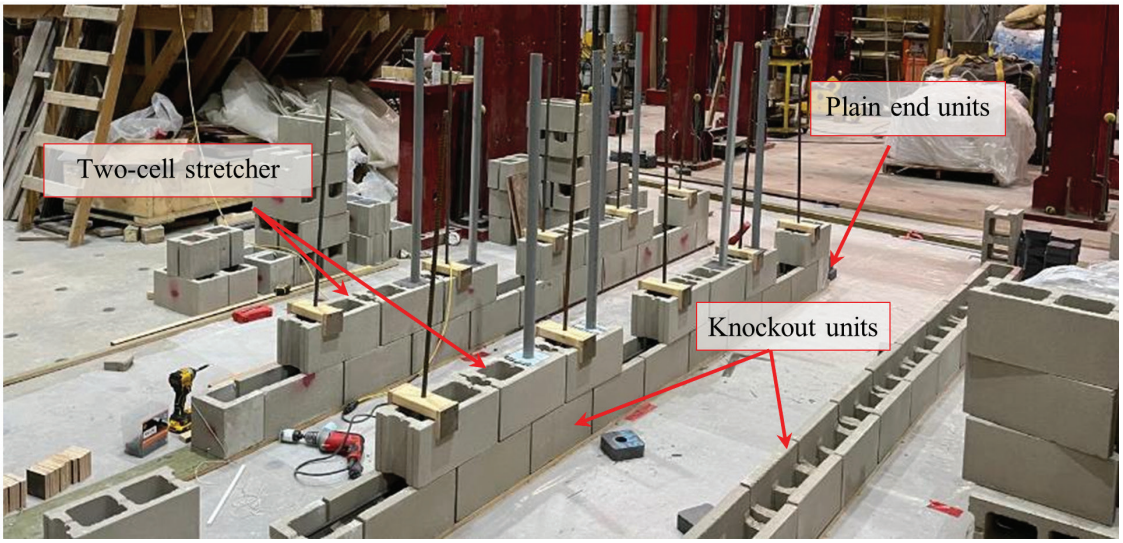

Figure 3. Masonry wall construction using three types of masonry blocks.

Horizontal reinforcement included two 10M (no. 3) bars in the bottom course to prevent cracking during handling and another pair in the third course, directly beneath the hollow-core slab, to form a standard bond beam. Complementing this, vertical wall reinforcement consisted of five 15M (no. 5) bars spaced at 800 mm (32 in.) on center, which were installed as part of the masonry wall construction within predetermined reinforced cells. During construction, the vertical bars were aligned and fixed, and the reinforced cells were fully grouted to provide a continuous load path at the slab-to-wall interface. The hollow-core slab units were then positioned such that the grouted shear key or keyway region coincided with the reinforced cell containing the dowel. This arrangement permitted direct engagement of the 10M integrity ties with the vertical reinforcement while ensuring grout consolidation around both the dowel and the connection bar at the interface.

Material properties

Masonry blocks had a compressive strength of 20 MPa (2.9 ksi), except for specimen EB-T-L-1 (first floor), which used 30 MPa (4.35 ksi) blocks to sustain increased axial demands. The grout used to fill the hollow blocks and slab cores satisfied the requirements of CSA A179-14 (R24), *Mortar and Grout for Unit Masonry*,[5] and ASTM C476-23, *Standard Specification for Grout for Masonry*.[6] The compressive strength of the grout was obtained through testing 51 mm (2 in.) cubes following ASTM C109-23, *Standard Test Method for Compressive Strength of Hydraulic Cement Mortars (Using 50 mm [2 in.] Cube Specimens)*.[7] The cube strengths on the testing day and at 28 days were 30.2 ± 3.1 MPa (4.4 ± 0.45 ksi) and 26.4 ± 3.1 MPa (3.8 ± 0.45 ksi), respectively. Type S mortar was used to build the masonry walls per CSA A179-14 (R24)[5] and ASTM C270-24, *Standard Specification for Mortar for Unit Masonry*,[8] yielding a compressive strength of 14.4 ± 2 MPa (2.1 ± 0.3 ksi) at 28 days.

Two sizes of steel reinforcing bars, 10M and 15M (no. 3 and 5), were used. Both bars exhibited a yield strength of 470 ± 8 MPa (68 ± 1 ksi), a yield strain of 2350 ± 40 με, and a modulus of elasticity of 199 GPa (28,800 ksi). The mechanical properties of the steel reinforcing bars were obtained by conducting standard tests per ASTM A370-24a, *Standard Test Methods and Definitions for Mechanical Testing of Steel Products*.[9]

The hollow-core slab segments were provided by a local precast concrete manufacturer with a target 28-day concrete compressive strength of 55 to 60 MPa (8 to 8.7 ksi).

Test setup and loading protocol

To evaluate the tensile performance of hollow-core-slab bar connections to masonry walls, a series of in-plane pull-away tests were conducted under controlled laboratory conditions. Each test was designed to simulate a realistic connection, with particular attention to replicating construction-level detailing and axial loading where applicable.

The wall specimens were supported on two hollow structural section (HSS) base members spaced 3500 mm (138 in.) apart. These base members were anchored to the laboratory's strong floor using high-strength prestressed bars, ensuring both vertical stability and rotational restraint during testing. Four vertical box-section steel columns were welded to the HSS base

members and braced laterally to resist overturning and support reaction forces generated during tensile loading (**Fig. 4**). To simulate continuity in a full-height masonry wall, an additional HSS beam was installed against the face of the lowest masonry course, limiting inward deflection and maintaining the integrity of the boundary conditions.

Axial tensile loading was applied to the hollow-core slab through a system of custom-fabricated clamping beams. These consisted of top and bottom HSS elements secured together by high-strength threaded rods passing through predrilled holes in the hollow-core slab. The lower clamping beam was supported on three steel link members with pinned-pinned ends and anchored to the laboratory strong floor. This setup permitted lateral translation of the slab during testing while carrying half of the slab's self-weight to mimic in-service support conditions (Fig. 4).

For intermediate-floor specimens (EB-T-L-5 and EB-T-L-1), a vertical compressive load was applied to the wall before tensile testing, representing the cumulative axial load from upper stories in a ten-story masonry building. This axial load was introduced using four bars pretensioned and anchored to external steel loading fixtures positioned at the top of the wall. The bars were tensioned to produce uniformly distributed loads of 250 kN/m (17.13 kip/ft) for the fifth-floor specimen and 450 kN/m (30.83 kip/ft) for the first-floor specimen. These values were derived from structural analysis reflecting tributary loads from the superstructure. Steel loading plates were used to ensure uniform load distribution and prevent localized crushing of the masonry.

After establishing the axial load (where applicable), monotonic pull-away loading was applied using a ±250 kN (56 kip) servo-controlled hydraulic actuator mounted to a rigid steel reaction frame bolted to the strong floor. The actuator was connected to the top clamping beam and operated at a constant displacement rate of 1.0 mm/min (0.04 in./min) until failure. For roof-level specimens (EB-T-L-R, EB-T-L-P,

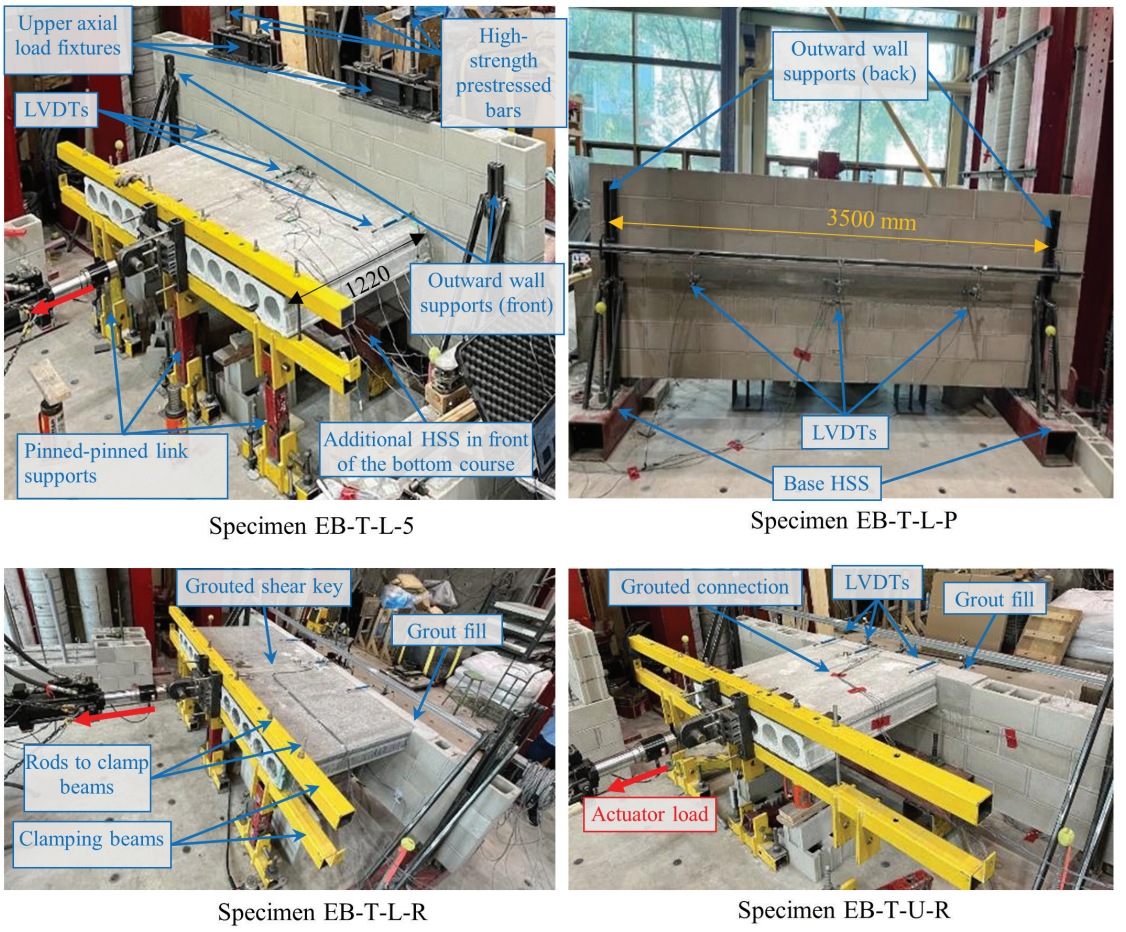

Figure 4. Details of the in-plane tensile test setup. Note: EB-T-L-P = end bearing configuration with tensile loading and an L-shaped bar connection with a parapet configuration; EB-T-L-R = end bearing configuration with tensile loading and an L-shaped bar connection at the roof level; EB-T-L-5 = end bearing configuration with tensile loading and an L-shaped bar connection at the fifth story; EB-T-U-R = end bearing configuration with tensile loading and a U-shaped bar connection at the roof level; HSS = hollow structural section; LVDT = linear variable displacement transducer. 1 mm = 0.0394 in.

EB-T-U-R, and EB-T-U-P), no axial preload was applied, as these conditions reflect minimal overburden load from above.

Test instrumentation

A comprehensive instrumentation plan was implemented to capture the mechanical response of the hollow-core-slab–to–masonry wall connections during testing. Relative displacements between the slab, grout, and wall were measured using three linear variable displacement transducers (LVDTs) mounted along the top surface of the hollow-core slab (Fig. 4). These LVDTs were positioned to monitor slip and separation at the interface between the slab and the wall. A second set of three LVDTs was installed at the rear face of the wall, aligned vertically with the LVDTs on the hollow-core slab, to track lateral deformation of the masonry wall. These sensors captured outward deflection of the wall due to tensile forces imposed by the slab (Fig. 4).

Strain behavior within the connection and surrounding reinforcement was monitored using electrical resistance strain gauges affixed to the integrity tie (connection bar) and the vertical wall reinforcement near the joint. Crack development at the connection zone and below the slab was tracked using Pi gauges (crack width indicators) installed at predefined critical locations.

Axial tensile force was measured by the built-in load cell of the hydraulic actuator. All measurements, including LVDT displacements, strain readings, crack widths, and applied loads, were continuously recorded using a computer-based data acquisition system throughout each test.

Crack initiation, propagation, and surface spalling were visually monitored during testing, with markings and high-resolution photographs documented at each stage to support postfailure analysis.

Test results and discussion

Mode of failure and cracking patterns

Figures 5 through **8** illustrate the failure modes and cracking patterns observed across all specimens. These patterns provide insight into the load transfer mechanisms and the performance

Figure 5. Test specimens at failure. Note: EB-T-L-R = end bearing configuration with tensile loading and an L-shaped bar connection at the roof level; EB-T-U-R = end bearing configuration with tensile loading and a U-shaped bar connection at the roof level.

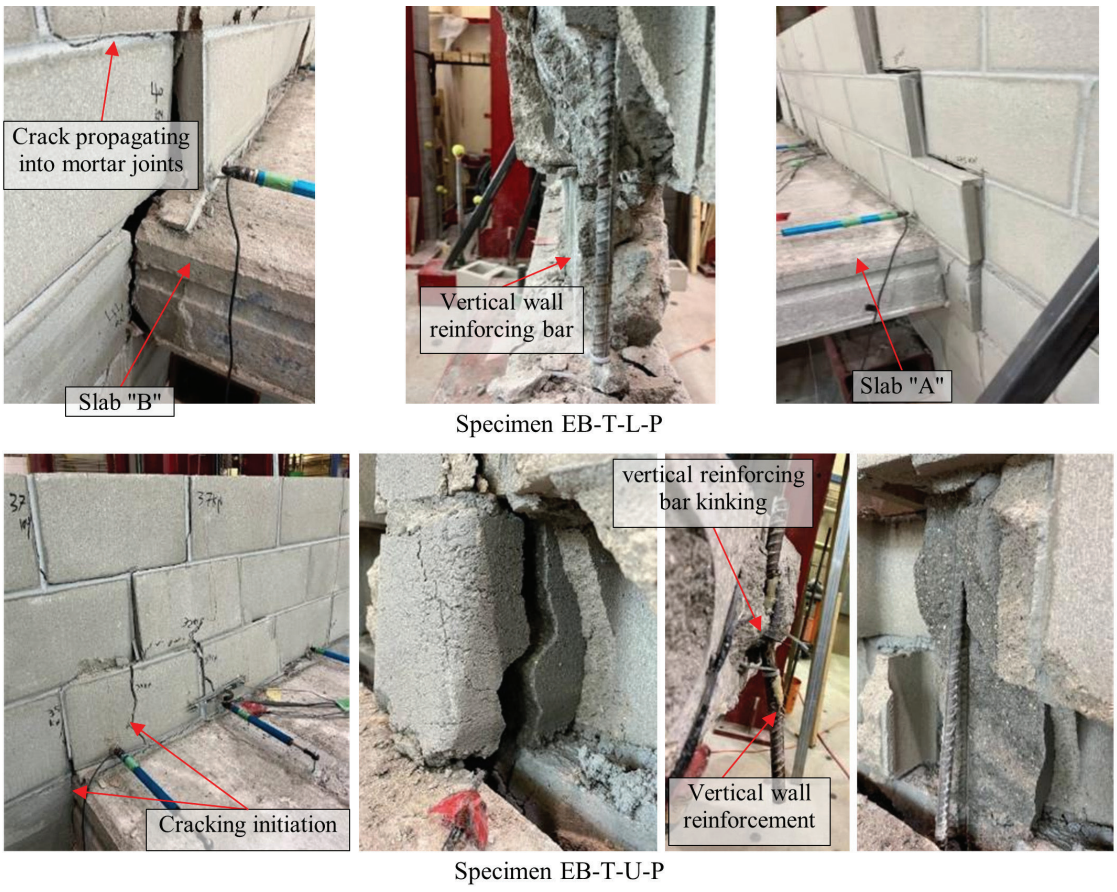

Figure 6. Test specimens at failure. Note: EB-T-L-P = end bearing configuration with tensile loading and an L-shaped bar connection with a parapet configuration; EB-T-U-P = end bearing configuration with tensile loading and a U-shaped bar connection with a parapet configuration.

of grout, integrity ties, and wall reinforcement under in-plane tensile loading. Test results are provided in **Table 2**.

Across all specimens, the response followed a consistent two-stage mechanism. Prior to peak load, resistance was dominated by shear transfer and shear friction mobilized at the grout-to-masonry interface and was strongly dependent on clamping. After interface cracking and local grout crushing, load redistributed to a secondary steel load path with the integrity tie acting in tension while wrapping behind the vertical wall reinforcement, which provided mechanical anchorage and grout-pocket confinement.

Cracking consistently initiated on the tension face of the masonry wall just below the hollow-core slab, indicating the onset of load transfer through the connection region. Vertical cracks were typically the first to form at relatively low load levels, signifying early engagement of the grout-to-masonry interface. As the applied load increased, diagonal cracks developed within the interface region, reflecting shear friction mobilization, an essential mechanism resisting slab pullout prior to full activation of the reinforcing bars. Peak loading in all specimens triggered pronounced grout cracking or crushing and interface separation. This loss of cohesion resulted in a sharp drop in load-carrying capacity, signaling the breakdown of shear friction. At this stage, the structural integrity of the system relied primarily on the integrity tie and vertical reinforcement, which were not significantly engaged until after cracking but proved effective in restraining excessive displacement and preventing full connection failure.

In specimens EB-T-L-R and EB-T-U-R, both bar shapes produced similar peak load capacities (25.4 and 25.7 kN [5.7 and 5.8 kip], respectively) but distinct failure mechanisms. In EB-T-L-R, diagonal cracking in the grout reduced the effective bearing length from the full 75 mm (3 in.) to approximately 15 mm (0.6 in.), initiating slab movement and engaging the L-shaped bar and wall vertical reinforcement. The L bar resisted slab pullout through anchorage in the grout until yielding occurred at the hook bend, partially deforming and opening the bar (Fig. 5). In contrast, EB-T-U-R exhibited local kinking of the vertical dowel at the interface with the U bar, which led to yielding and eventual crushing of the surrounding masonry blocks (Fig. 5). In both cases, the rein-

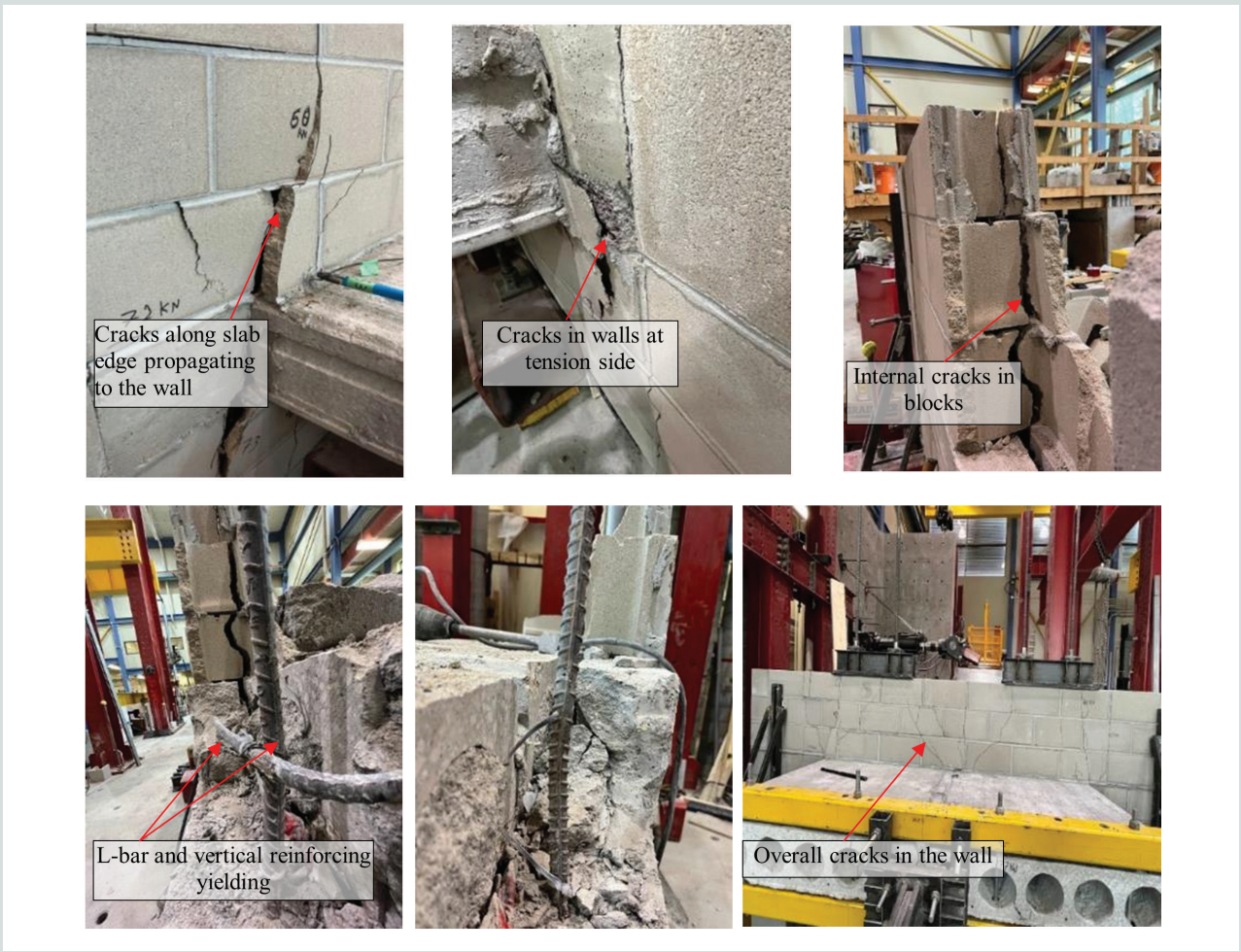

Figure 7. The mode of failure for specimen EB-T-L-5 (end bearing configuration with tensile loading and an L-shaped bar connection at the fifth story).

forcing system limited displacement postpeak and preserved system continuity.

The addition of a parapet above the hollow-core slab in specimens EB-T-L-P and EB-T-U-P produced notably higher resistance than the roof condition. This improvement is attributed primarily to greater development of the vertical wall reinforcement above and below the slab elevation, which reduced cantilever-type bending action of the 15M bar and distributed tension forces into a larger region of the wall. In EB-T-L-P, initial cracking was observed at 28 kN (6.3 kip), followed by vertical face cracking and upward propagation through mortar joints at 42 kN (9.4 kip). The specimen reached a peak load of 57 kN (12.8 kip), after which slab B began to separate while slab A remained engaged with the wall (Fig. 6). Cracking of masonry beneath the slab and within the shear key was evident. The integrity tie and vertical reinforcement restrained full pullout, allowing the system to exhibit controlled postpeak behavior. For EB-T-U-P, cracking initiated along the grout–to–hollow-core-slab interface at 33 kN (7.4 kip), peaking at 38.5 kN (8.6 kip) with observed slab separation and grout splitting (Fig. 6). Kinking of the U bar caused compressive strains in the dowel, contrasting with the tensile-dominated failure in EB-T-L-P and highlighting the influence of bar geometry on mode of failure.

Intermediate-floor specimens EB-T-L-5 and EB-T-L-1, subjected to axial compression, exhibited delayed and more distributed cracking. In EB-T-L-5, initial internal cracking occurred at 45 kN (10.1 kip) and intensified with wall face cracking at 60 kN (13.5 kip), ultimately reaching a peak load of 88.5 kN (19.9 kip) (Fig. 7). Spalling developed above slab A, while slab B detached due to combined shear failure and bar yielding.

Specimen EB-T-L-1 demonstrated a similar but more abrupt failure progression. Cracks initiated at 60 kN (13.5 kip) and propagated toward the slab edges, with a major fracture forming above the grout interface at 72 kN (16.2 kip). The peak load of 90 kN (20.2 kip) was accompanied by yielding in both the L bar and vertical wall reinforcement (Fig. 8). Although axial compression improved connection capacity, it also amplified vertical cracking, leading to partial disengagement of masonry units above the slab and affecting wall integrity.

Figure 8. The mode of failure for specimen EB-T-L-1 (end bearing configuration with tensile loading and an L-shaped bar connection at the first story).

Across all tests, ultimate resistance was primarily governed by shear friction at the grout-to-masonry interface. Following peak load and major cracking, the integrity ties—though not designed to carry the full load—became critical in limiting further displacement and preserving overall structural function. Continued load resistance beyond the peak demonstrated the ability of the reinforcing system to maintain composite behavior and delay collapse.

Compared with details commonly used in eastern Canada practice, where ties are postinstalled into drilled masonry holes using dry-fit or adhesive methods, the western Canada wrapped-bar detail provides a more robust postpeak load path by introducing steel-to-steel anchorage through the vertical wall reinforcement and confining the grout pocket. Previous tests on postinstalled ties[3] reported failure modes including tie-bar pullout, grout splitting, and masonry block fracture, which resulted in loss of bearing. In contrast, the present tests demonstrated that wrapped ties maintained integrity after interface cracking, transferring tensile demand into the vertical wall reinforcement and restraining grout-pocket splitting, thereby sustaining residual capacity.

These findings suggest that failure in hollow-core-slab–to–wall bar connections is not characterized by sudden loss of support but rather by gradual disengagement, mitigated by the interaction between integrity ties and vertical reinforcement. This composite action contributed to ductile system behavior and underscores the importance of proper detailing in enhancing postpeak resilience under in-plane tensile loading.

Connection load capacity

The capacity of end-bearing bar connections between hollow-core slab segments and masonry walls was evaluated under in-plane tensile loading to verify adequacy relative to North American codes and understand the governing strength mechanisms. All specimens employed 10M (no. 3) deformed steel bars (11.3 mm [0.44 in.] diameter, 100 mm^2 [0.16 $in.^2$] cross-sectional area) with a nominal yield strength of 400 MPa (58 ksi), corresponding to a theoretical tensile capacity of 40.0 kN (9.0 kip) per bar. For the U-shaped bars, which embed both legs within the grout, the theoretical tensile capacity could be approximated as 80.0 kN (18.0 kip), assuming full anchorage and strain compatibility; however,

Table 2. Test results

Specimen ID	Cracking load, kN	Peak load, kN	Yielding load, kN		Strain at peak load, με		Slab-to-wall interface relative displacement, mm	Mode of failure
			Vertical bar	Connection bar	Vertical bar	Connection bar		
EB-T-L-R	16.3	25.4	18.7	n/a	495.3	579.9	32.6	Masonry block face spalling and vertical bar yielding
EB-T-L-P	33.4	57.0	45.3	n/a	914.7	50.5	27.9	Loss of support, masonry block face spalling, and vertical bar yielding
EB-T-L-5	60.4	88.5	43.4	43.2	131.2	251.3	31	Masonry block face spalling, interior splitting in masonry blocks, and vertical wall reinforcement yielding
EB-T-L-1	60.6	90.0	50.5	80.0	202.2	31.7	32.5	Interior splitting into masonry blocks and reinforcing bars yielding
EB-T-U-R	18.2	25.7	20.1	n/a	373.4	43.4	45.1	Masonry block face spalling and vertical bar yielding
EB-T-U-P	32.3	38.0	35.6	n/a	716.3	283.8	28.1	Grout splitting and vertical bar yielding

Note: EB-T-L-P = end bearing configuration with tensile loading and an L-shaped bar connection with a parapet configuration; EB-T-L-R = end bearing configuration with tensile loading and an L-shaped bar connection at the roof level; EB-T-L-1 = end bearing configuration with tensile loading and an L-shaped bar connection at the first story; EB-T-L-5 = end bearing configuration with tensile loading and an L-shaped bar connection at the fifth story; EB-T-U-P = end bearing configuration with tensile loading and a U-shaped bar connection with a parapet configuration; EB-T-U-R = end bearing configuration with tensile loading and a U-shaped bar connection at the roof level. 1 mm = 0.0394 in.; 1 kN = 0.225 kip.

practical factors, such as uneven strain distribution or partial development, often limit this idealized capacity.

Standard hollow-core-slab–to–masonry wall end-bearing connections typically use one 10M (no. 3) bar per grout key, spaced at 1220 mm (48 in.). Considering CSA A23.3:24[1] and a strength-reduction factor ϕ of 0.85, minimum factored tie demands correspond to nominal per-bar requirements of 7.2 kN (1.6 kip) for single-story and 20.1 kN (4.5 kip) for multistory structures. ACI 318-25[2] specifies nominal minimum tensile strengths of 5.4 kN (1.2 kip) per bar for diaphragm connections and 26.8 kN (6.0 kip) per bar for bearing-wall structures three stories or taller. All measured peak loads satisfied the CSA A23.3:24 minimum tie requirements for diaphragm connections. However, the peak loads of EB-T-L-R and EB-T-U-R did not reach the 26.8 kN (6.0 kip) nominal tensile strength requirement prescribed by ACI 318-25 for bearing-wall structures three stories or taller.

The test results, summarized in **Fig. 9**, show that all specimens exceeded the minimum structural integrity requirements prescribed by CSA A23.3:24 and ACI 318-25. However, the roof-level specimens without parapets (EB-T-L-R and EB-T-U-R), with peak loads of 25.4 and 25.7 kN (5.7 and 5.8 kip), respectively, did not satisfy the ACI 318-25 minimum tensile strength requirement for bearing-wall structures three stories or taller. These capacities were predominantly controlled by shear friction resistance at the grout-to-masonry interface rather than the full yield capacity of the steel bars, underscoring the interface as the principal load transfer mechanism in such connections under tension without axial compression.

The addition of a parapet condition both significantly enhanced load capacity and reduced interface separation compared with EB-T-L-R. This improvement is attributed mainly to enhanced development and engagement of the vertical reinforcement above and below the slab elevation, which improved confinement and load distribution at the grout pocket. EB-T-L-P achieved a peak load of 57.0 kN (12.8 kip), while EB-T-U-P reached 38.0 kN (8.5 kip), representing increases of 124% and 50%, respectively, compared with their nonparapet roof counterparts. The two-slab configuration of EB-T-L-P facilitated greater contact area with the grout and vertical reinforcement, further improving load distribution and enhancing the mechanical interlock across the joint. While the U bar has a higher theoretical capacity, the single-slab geometry and

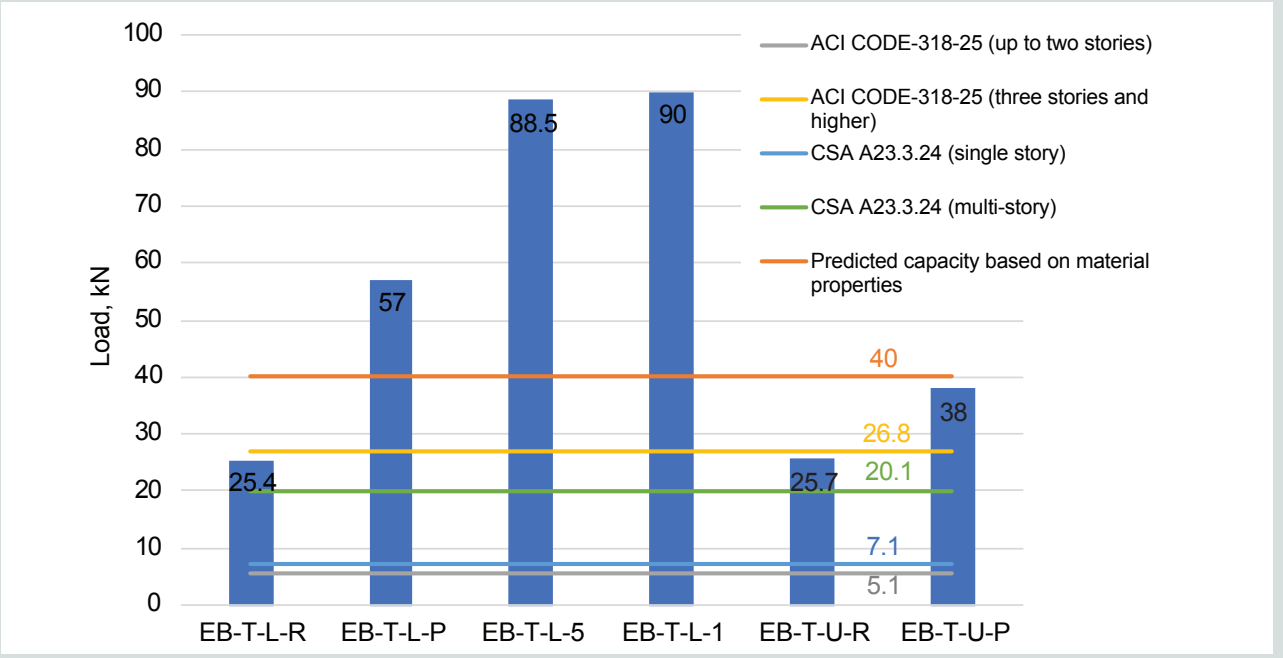

Figure 9. Effect of different parameters on the capacity of the specimens. Note: ACI CODE-318-25 = American Concrete Institute's *Building Code for Structural Concrete—Code Requirements and Commentary*; CSA A23.3:24 = Canadian Standards Association (CSA) Group's *Design of Concrete Structures*; EB-T-L-P = end bearing configuration with tensile loading and an L-shaped bar connection with a parapet configuration; EB-T-L-R = end bearing configuration with tensile loading and an L-shaped bar connection at the roof level; EB-T-L-1 = end bearing configuration with tensile loading and an L-shaped bar connection at the first story; EB-T-L-5 = end bearing configuration with tensile loading and an L-shaped bar connection at the fifth story; EB-T-U-P = end bearing configuration with tensile loading and a U-shaped bar connection with a parapet configuration; EB-T-U-R = end bearing configuration with tensile loading and a U-shaped bar connection at the roof level. 1 kN = 0.225 kip.

strain compatibility limitations may have restricted its effectiveness compared with the dual-slab L-bar configuration.

The highest capacities were observed in intermediate-floor specimens subjected to significant axial compression. EB-T-L-5 and EB-T-L-1 reached 88.5 and 90.0 kN (19.9 and 20.2 kip), increases of about 55% and 58% over EB-T-L-P, demonstrating axial load's strong role in improving interface clamping, delaying grout cracking, and mobilizing embedded reinforcement. The minimal difference between EB-T-L-5 and EB-T-L-1 suggests that beyond a certain axial load threshold, capacity gains plateau, likely due to material limits in grout and masonry. This is reflected in **Fig. 10**, where load–displacement curves plateau near predicted material limits, indicating that further axial load does not significantly enhance tensile resistance.

Across all specimens, the vertical reinforcement embedded within the masonry wall—a defining feature of western Canada practice—was critical in maintaining load path continuity. In western Canada practice, tensile integrity forces are transferred to the wall within the plane of the hollow-core slab diaphragm through slab/grout-key reinforcement that engages the vertical reinforcing bars in the wall. The combined action of vertical reinforcement and integrity ties distributes tensile demands beyond the interface, forming a continuous and redundant structural system that enhances strength, ductility, and overall connection integrity. In contrast, the eastern Canada L-bar detail transfers tensile integrity forces to the wall below through shear and bending of the reinforcing grout joint bar, resulting in a more flexible response under direct tension at the slab-to-wall joint. Maintaining the tensile force transfer within the diaphragm plane provides a stiffer slab-to-wall connection response under in-plane tension.

In summary, all tested configurations satisfied the CSA and ACI minimum structural integrity requirements except the roof-level specimens without parapets (EB-T-L-R and EB-T-U-R), which did not meet the ACI 318-25 tensile strength requirements for bearing-wall structures three stories or taller. Nevertheless, the results confirm that properly detailed end-bearing connections—particularly those incorporating axial compression and vertical wall reinforcement—can deliver robust, ductile, and code-compliant performance under in-plane tensile loading.

Reinforcement strain analysis

The progression of strain in the connection bars and vertical wall reinforcement provides crucial insight into the load transfer mechanisms and postpeak behavior of the end-bearing hollow-core-slab–to–masonry wall connections. As observed in the previous sections, the initial resistance of each specimen was dominated by shear transfer across the grout-to-masonry interface, followed by progressive engagement of embedded reinforcement after grout degradation. **Figures 11** and **12** show the load–strain response of

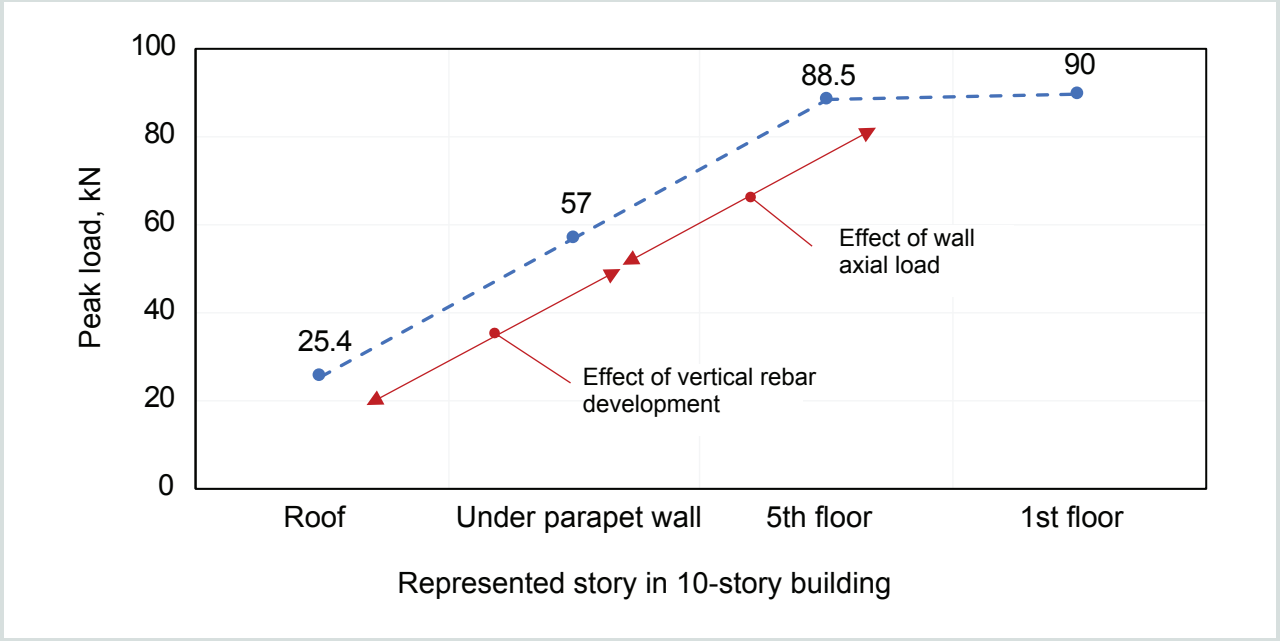

Figure 10. Effect of vertical reinforcing bar development and number of floors on connection capacity. Note: 1 kN = 0.225 kip.

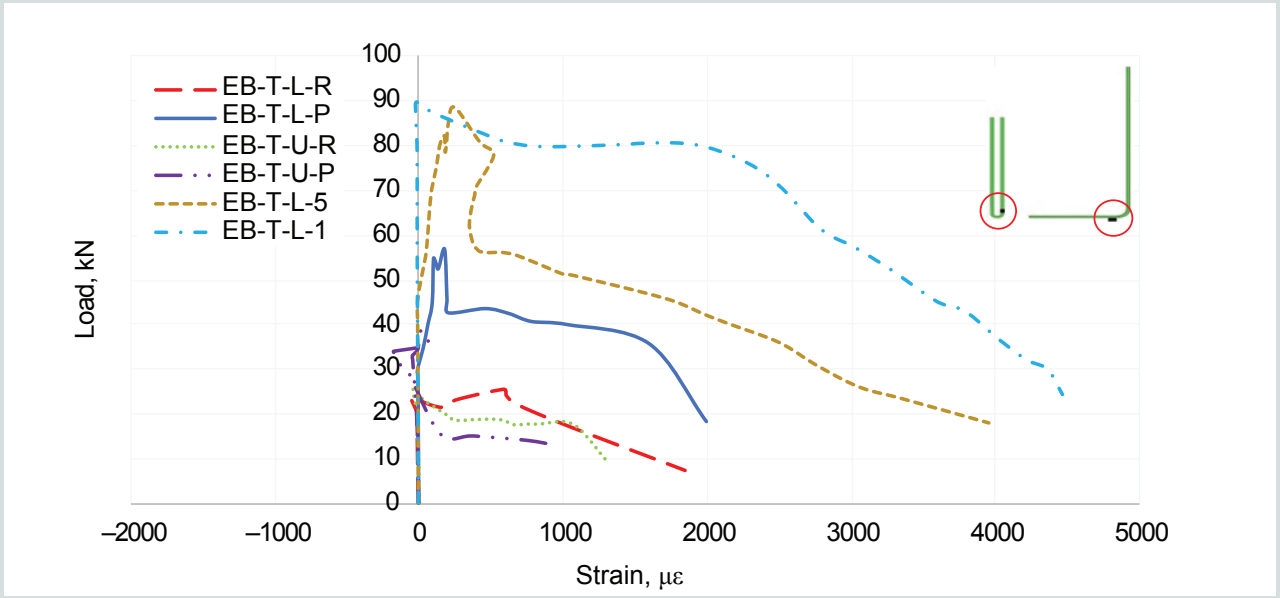

Figure 11. Strain versus load in connection reinforcing bar. Note: EB-T-L-P = end bearing configuration with tensile loading and an L-shaped bar connection with a parapet configuration; EB-T-L-R = end bearing configuration with tensile loading and an L-shaped bar connection at the roof level; EB-T-L-1 = end bearing configuration with tensile loading and an L-shaped bar connection at the first story; EB-T-L-5 = end bearing configuration with tensile loading and an L-shaped bar connection at the fifth story; EB-T-U-P = end bearing configuration with tensile loading and a U-shaped bar connection with a parapet configuration; EB-T-U-R = end bearing configuration with tensile loading and a U-shaped bar connection at the roof level. 1 kN = 0.225 kip.

the connection bars and vertical reinforcement, respectively, with peak values summarized in Table 2.

For the connection bar, strain measurements were taken after the bend to capture local variations, while vertical bar strains were recorded at the masonry wall's top surface.

Connection bar strain behavior

During the early stages of loading, the connection bars in all specimens exhibited negligible strain, indicating that the tensile load was initially resisted by interface shear and slab bearing. This observation is consistent with the cracking patterns dis-

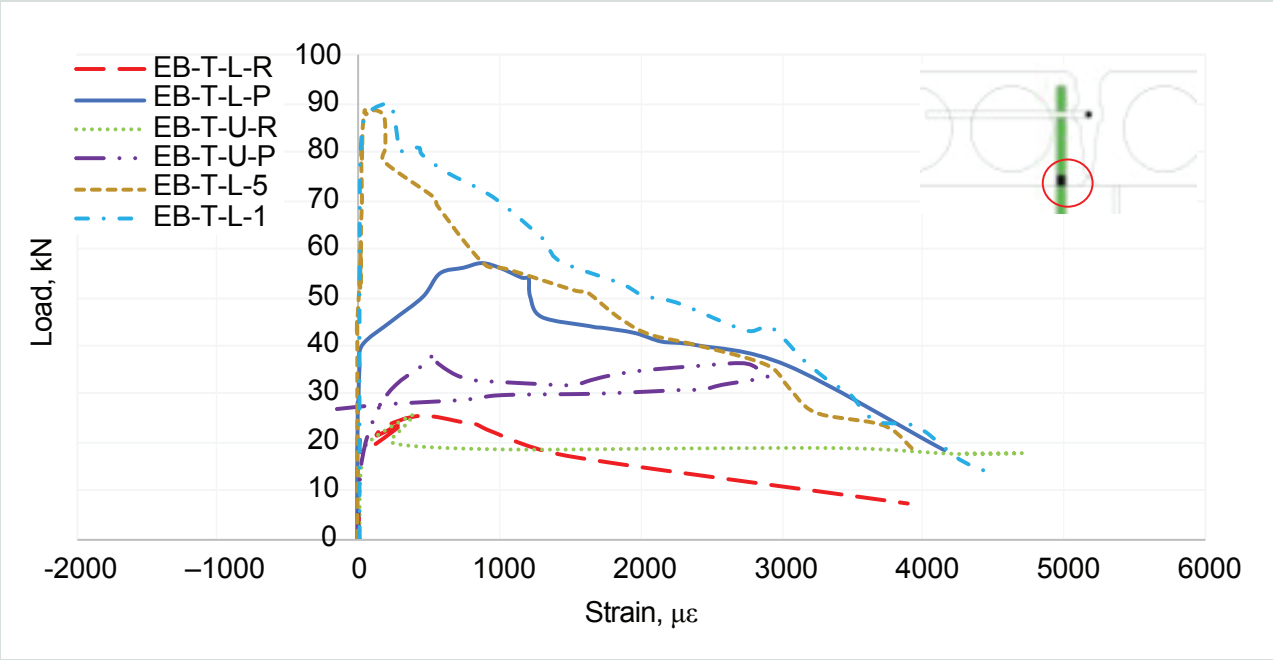

Figure 12. Strain versus load in vertical reinforcing bar. Note: EB-T-L-P = end bearing configuration with tensile loading and an L-shaped bar connection with a parapet configuration; EB-T-L-R = end bearing configuration with tensile loading and an L-shaped bar connection at the roof level; EB-T-L-1 = end bearing configuration with tensile loading and an L-shaped bar connection at the first story; EB-T-L-5 = end bearing configuration with tensile loading and an L-shaped bar connection at the fifth story; EB-T-U-P = end bearing configuration with tensile loading and a U-shaped bar connection with a parapet configuration; EB-T-U-R = end bearing configuration with tensile loading and a U-shaped bar connection at the roof level. 1 kN = 0.225 kip.

cussed earlier, where vertical and diagonal cracks developed beneath the hollow-core slab before any significant bar engagement occurred. Concurrently, modest strain was recorded in the vertical reinforcement—particularly in specimens with L-shaped bars—suggesting that the axial load was partially redirected from the slab through the grout and into the wall height, activating the dowels before the connection bar fully engaged.

As loading progressed and interface cracking widened, the load demand shifted to the reinforcing bars. This transition was marked by a rapid increase in bar strain, most notably in the connection bars of specimens with L-shaped configurations. In specimens such as EB-T-L-R and EB-T-L-P, the straightening of the hooked bar initiated localized bending and tension, with strain rising from approximately 500 με preyield to over 1800 με postpeak. The connection bars became the primary load-carrying element after grout shear resistance was lost, consistent with the observed drop in peak load and the onset of bar-controlled response.

Bar geometry had a significant impact on both strain development and the overall load path. L-shaped bars, used in four of the six specimens, were anchored in the grout with a single leg. This geometry created a hinge-like behavior, where the bar attempted to straighten under tension, applying force to the vertical wall reinforcement and inducing outward displacement of the wall face. The response was concentrated and directional, with peak strain values reflecting full bar engagement following grout cracking.

By contrast, the U-shaped bar specimens (EB-T-U-R and EB-T-U-P) exhibited a more distributed and stable strain response. With both legs embedded in the grout, the U-bar configuration provided improved symmetry in load transfer and a broader anchorage region. Peak strain remained below yield in both cases, 1330 and 920 με, indicating that the bars did not fully develop their theoretical capacity. This could be attributed to partial engagement of the two legs, strain incompatibility, or localized grout degradation near one leg. Nonetheless, the U-bar configuration promoted smoother stress redistribution and contributed to reduced postpeak displacement compared with the more abrupt transitions in the L-bar specimens.

Specimens subjected to vertical axial compression (EB-T-L-5 and EB-T-L-1) showed the most pronounced connection bar strains, reaching 4000 and 4500 με, respectively, well beyond the yield point. Axial load delayed the onset of grout cracking and maintained the integrity of the grout-to-bar interface, enabling a more progressive engagement of the bar. In EB-T-L-1, the presence of higher axial compression allowed for longer grout-to-bar interaction and smoother strain accumulation, whereas in EB-T-L-5, a sudden strain surge followed grout fracture, leading to a sharper postpeak response.

Strain readings in the vertical reinforcement revealed its crucial role in sustaining the load path after interface degradation. In all specimens, the vertical wall reinforcement yielded during testing, particularly in the L-bar configurations, where vertical reinforcement strains increased in parallel with bar

straightening and wall rotation. The strain was distributed along the wall reinforcement height, confirming that the load was transmitted beyond the immediate connection zone and into the full height of the wall. This behavior supports the findings discussed in the "Connection load capacity" section of this paper, where vertical reinforcement acted as a distributed anchorage system, extending and stabilizing the load path beyond the slab level. This behavior was most pronounced in specimens where the 15M (no. 5) vertical reinforcement was fully developed above and below the slab elevation (for example, the parapet and intermediate-floor configurations), enabling a larger portion of the wall system to participate in resisting the tensile demand.

In U-bar specimens, the strain profile in the dowels was more localized, with signs of kinking and bending near the wrap intersection. Although this configuration reduced global wall movement and bar rotation, it introduced concentrated stresses at the dowel bend. Even so, the U-bar geometry ensured a more balanced engagement of the reinforcement system, which helped prevent premature yielding.

The reinforcement strain behavior confirms that the tensile capacity of the system is not solely dependent on the bar itself but on the coordinated interaction between grout integrity, bar geometry, and vertical reinforcement. L-shaped bars provided high capacity when paired with axial load and strong dowel anchorage but exhibited more abrupt transitions after grout failure. U bars offered improved stress distribution but may not reach their full theoretical strength without strain compatibility across both legs.

Importantly, the presence of vertical wall reinforcement, standard in western Canada detailing, proved essential. It provided an extended and resilient load path that reduced the likelihood of brittle failure and enhanced the postpeak ductility of the system. Compared with practices that omit vertical wall reinforcement, the integrated reinforcement strategy observed here offered superior energy dissipation, strain redistribution, and structural redundancy, critical features in designing safe, resilient diaphragm-to-wall connections.

Displacement of the slabs and the wall

The relative displacement behavior between hollow-core slabs and masonry walls under in-plane tensile loading offers critical insight into the progression of load transfer, interface failure, and the ductility of the overall diaphragm-to-wall connection. **Figures 13** and **14** illustrate the slab-to-grout interface separation and the corresponding lateral wall deflections, respectively, across all specimen configurations. In accordance with CSA A23.3:24, a multistory factored tie demand of 20.1 kN (4.5 kip) per bar was considered. Given an initial bearing length of 76 mm (3 in.), the maximum allowable lateral separation to maintain the minimum required bearing length of 50 mm (2 in.) is 26 mm (1 in.) (that is, 76 – 50 = 26 mm). The experimental results indicate that all specimens reached the load level of 20.1 kN at displacement levels well

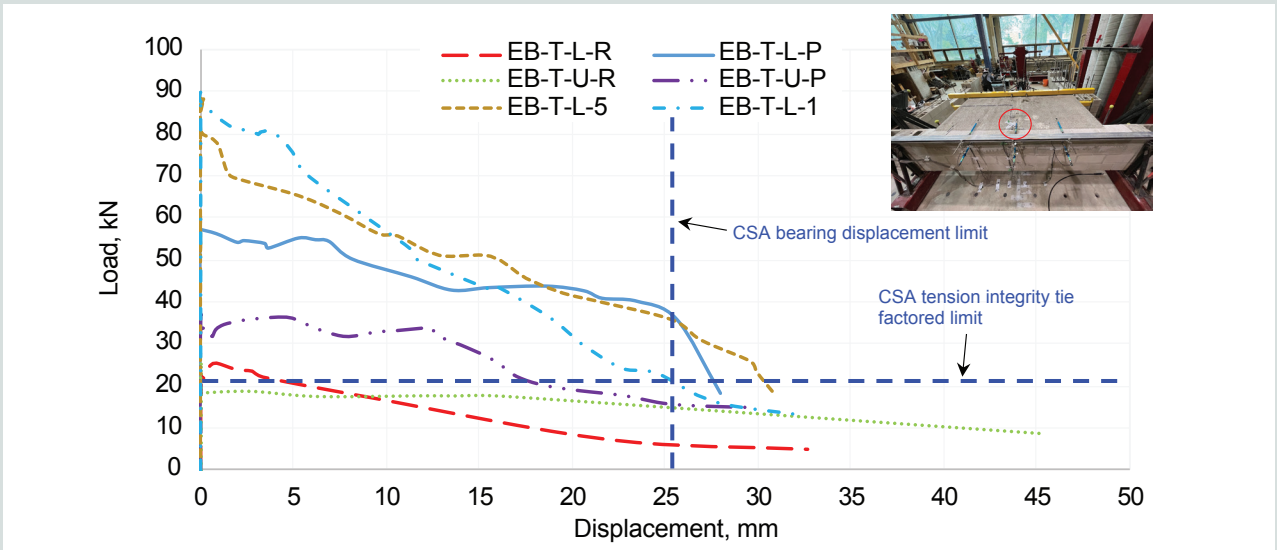

Figure 13. Relative displacement between slabs and grout interface at top of wall. Note: Displacements up to peak load are small (typically submillimeter) and therefore are not visually distinct at the scale of this figure; the plot is intended to highlight postpeak interface separation and residual load behavior. CSA = Canadian Standards Association (CSA) Group's *Design of Concrete Structures*; EB-T-L-P = end bearing configuration with tensile loading and an L-shaped bar connection with a parapet configuration; EB-T-L-R = end bearing configuration with tensile loading and an L-shaped bar connection at the roof level; EB-T-L-1 = end bearing configuration with tensile loading and an L-shaped bar connection at the first story; EB-T-L-5 = end bearing configuration with tensile loading and an L-shaped bar connection at the fifth story; EB-T-U-P = end bearing configuration with tensile loading and a U-shaped bar connection with a parapet configuration; EB-T-U-R = end bearing configuration with tensile loading and a U-shaped bar connection at the roof level. 1 mm = 0.0394 in.; 1 kN = 0.225 kip.

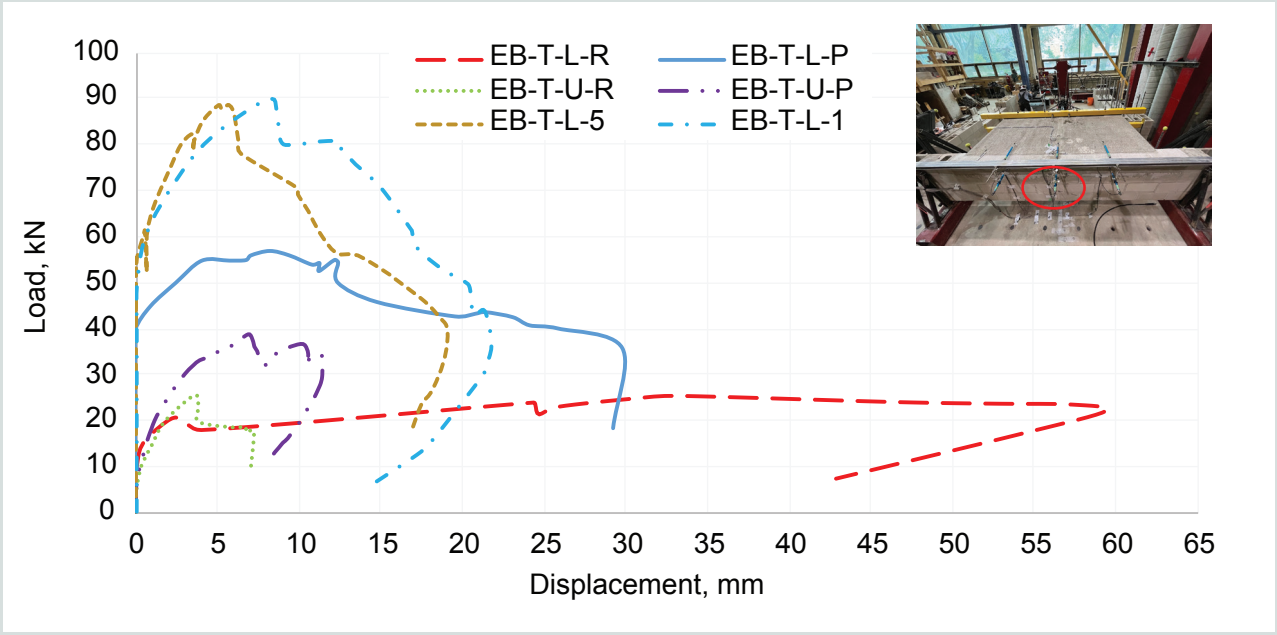

Figure 14. Wall deflection at connection zone. Note: EB-T-L-P = end bearing configuration with tensile loading and an L-shaped bar connection with a parapet configuration; EB-T-L-R = end bearing configuration with tensile loading and an L-shaped bar connection at the roof level; EB-T-L-1 = end bearing configuration with tensile loading and an L-shaped bar connection at the first story; EB-T-L-5 = end bearing configuration with tensile loading and an L-shaped bar connection at the fifth story; EB-T-U-P = end bearing configuration with tensile loading and a U-shaped bar connection with a parapet configuration; EB-T-U-R = end bearing configuration with tensile loading and a U-shaped bar connection at the roof level. 1 mm = 0.0394 in.; 1 kN = 0.225 kip.

below this allowable limit (Fig. 13). This demonstrates that adequate bearing was preserved at the CSA code-specified factored demand.

Interface separation and load transfer mechanisms

During the early loading stages, all specimens exhibited minimal relative movement between the slab and grout interface, indicating full composite action of the slab–grout–wall assembly. This cohesive behavior persisted up to peak load. This early-stage stiffness is consistent with observations from reinforcement strain data and cracking patterns, where the connection primarily resisted load through shear at the grout-to-masonry interface. The vertical reinforcement embedded in the grout pocket contributed significantly during this phase by maintaining seating length and promoting distributed force transfer into the wall height.

After interface cracking initiated, typically just before peak load, relative displacement increased as the connection transitioned from shear-dominated behavior to reinforcement-controlled resistance. At this stage, the connection bar and vertical wall reinforcement became increasingly engaged, accommodating deformation while limiting full detachment. For example, EB-T-L-R showed a peak interface displacement of 0.84 mm (0.03 in.), while EB-T-L-P (representing the parapet condition with developed vertical reinforcement above and below the slab elevation) displayed smaller peak displacement, demonstrating the stabilizing effect of vertical bar development and engagement of a larger area of the wall for connection resistance.

U-bar specimens (EB-T-U-R and EB-T-U-P) consistently recorded lower peak displacements compared with their L-bar counterparts due to the symmetrical anchorage and dual-leg engagement within the grout. This improved strain compatibility and delayed interface separation, further confirmed the U bar's superior control of deformation under tensile loading.

The postpeak response highlights each configuration's ability to maintain load resistance at large deformations, a key indicator of ductility and connection robustness. Intermediate-floor specimens (EB-T-L-5 and EB-T-L-1), tested under high axial loads, exhibited the most favorable displacement behavior. After reaching peak capacities around 90 kN (20.2 kip), both maintained substantial residual strength (approximately 22 kN [4.9 kip]) up to displacements of 30 to 35 mm (1.2 to 1.4 in.). These residual loads align closely with the minimum tensile capacity required by CSA (20.1 kN [4.5 kip]) for multistory construction, demonstrating that the integrity ties and vertical wall reinforcement continued to provide a stable load path even after interface degradation.

Among roof-level specimens without parapets, EB-T-U-R outperformed EB-T-L-R in both residual strength and deformation capacity. The U-bar specimen sustained approximately 17.5 kN (3.9 kip) beyond 25 mm (1.0 in.) displacement, whereas the L-bar counterpart dropped to 18 kN (4.0 kip) at just 10 mm (0.4 in.) displacement. This stark contrast underscores the influence of bar geometry on load redistribution and deformation resistance: U-shaped bars provided a more balanced and gradual

postpeak response, while L bars experienced earlier disengagement due to asymmetric load transfer and concentrated strain.

The addition of parapet walls significantly enhanced both load capacity and displacement control, and specimens displayed reduced interface separation compared with EB-T-L-R. This improvement is attributed mainly to enhanced development and engagement of the vertical reinforcement above and below the slab elevation, which improved confinement and load distribution at the grout pocket. Any parapet self-weight clamping is considered secondary. The postpeak force–displacement response for EB-T-L-P and EB-T-U-P showed slower degradation, attributed primarily to improved development and engagement of the vertical reinforcement and increased confinement at the connection zone. The contribution of parapet self-weight to axial clamping is comparatively modest.

Wall deflection and system integrity Lateral deflection of the masonry wall at the connection zone provides additional context to the interface performance (Fig. 14). EB-T-L-R, which lacked vertical restraint from engagement of parapet vertical reinforcement above the hollow-core slabs, showed the highest wall deflection at failure, 60 mm (2.36 in.), consistent with its abrupt postpeak behavior. By contrast, EB-T-L-P's peak deflection was limited to 30 mm (1.18 in.), reflecting a reduction attributed primarily to improved development and engagement of the vertical reinforcement above and below the slab elevation, which distributed the tensile demand into a larger portion of the wall and reduced localized rotation.

Bar geometry again proved influential. L-bar specimens, such as EB-T-L-R and EB-T-L-P, recorded wall deflections of 33 and 8.2 mm (1.3 and 0.3 in.), respectively, while U-bar specimens EB-T-U-R and EB-T-U-P showed significantly smaller deflections, 3.8 and 7.2 mm (0.15 and 0.28 in.). This difference reinforces the stabilizing influence of the U bar's dual-leg embedment, which better confined the grout pocket and distributed load across the wall face.

Interestingly, despite being subjected to the highest loads, intermediate-floor specimens EB-T-L-5 and EB-T-L-1 maintained modest wall deflections of 5.6 and 8.5 mm (0.22 and 0.33 in.), respectively. The presence of significant axial compression not only enhanced peak strength but also constrained out-of-plane wall movement, supporting the notion that vertical loading fosters composite action and mitigates postpeak instability.

The displacement behavior across all specimens confirms that axial loading, bar geometry, and vertical wall reinforcement are key to achieving ductile, code-compliant, and damage-tolerant diaphragm-to-wall connections. The ability of the connections to sustain loads well beyond peak and at large deformations validates the effectiveness of end-bearing bars and grout keys when detailed properly. In particular, specimens with axial compression and continuous vertical reinforcement, representative of western Canada practice, demonstrated improved performance in terms of both strength retention and displacement control, supporting their implementation in resilient precast concrete systems.

Conclusion

This study investigated the tensile performance of end-bearing bar connections between hollow-core slabs and masonry walls under in-plane pull-away loading. Based on the results, the following conclusions are drawn:

- The grout-to-masonry interface was identified as the primary load-resisting mechanism prior to grout cracking. Peak load capacity across all specimens was governed by the shear friction mobilized at this interface rather than the full tensile strength of the embedded reinforcing bars. This highlights the need for interface integrity in diaphragm-to-wall connections.

- Although both L-shaped and U-shaped bars achieved comparable peak loads, the U-bar configurations exhibited more stable postpeak behavior, reduced displacement, and lower strain concentration. The dual-leg anchorage of the U bar promoted better load distribution and minimized premature detachment, which were particularly beneficial where axial loads were limited.

- The inclusion of vertical reinforcement within the masonry wall, common in western Canada practice, proved critical to maintaining a continuous load path after interface cracking. It confined the grout, redistributed forces, and facilitated a ductile postpeak response. Compared with eastern Canada practice, where integrity ties are commonly postinstalled into drilled masonry holes using dry-fit or adhesive methods and rely primarily on bond, the western Canada detail evaluated in this study, where the integrity tie mechanically engaged the vertical wall reinforcement (that is, wrapped or looped around the vertical bar) helped maintain a continuous load path after interface cracking and preserved residual capacity at large deformations.

- Axial loading, whether from simulated upper stories or parapet dead loads, significantly increased connection capacity and improved postpeak resilience. The clamping effect delayed grout cracking, enhanced engagement of the embedded bars, and reduced both slab-to-grout separation and wall deflection. However, the capacity gain diminished beyond five stories, suggesting a saturation effect in which increased axial load yields marginal improvements.

- All connections with extended wall above the slab level (that is, intermediate floors and roof with parapet) satisfied minimum tensile strength requirements of both CSA A23.3:24 and ACI 318-25. Roof-level connections without parapets did not achieve the ACI 318-25 requirements for structures of three stories or taller. Despite this fact, post-peak response indicated that residual strengths for nonroof configurations generally

remained above the governing code thresholds, demonstrating the overall robustness of properly detailed end-bearing bar connections.

- Despite significant cracking and displacement beyond peak load, none of the specimens experienced full pullout of the slab. Integrity ties and vertical reinforcement ensured continued engagement and provided a secondary load path, underscoring the redundancy and resilience of the tested connection systems.

- L-shaped bars developed higher postpeak strain levels, often leading to tensile-induced bending of the vertical wall reinforcement due to their unidirectional pull. This behavior produced elevated strain concentrations in both the connection bar and wall reinforcement. Conversely, U-shaped bars exhibited more favorable load distribution, with reduced strain localization and compressive bending of the dowel through their wrapped geometry. This demonstrates that bar configuration plays a key role in stress redistribution and postpeak stability.

Acknowledgments

The authors gratefully acknowledge the financial support from the Canadian Precast/Prestressed Concrete Institute, the Natural Sciences and Engineering Research Council of Canada, and the Canadian Standards Association. In-kind contributions from Multicrete Precast Inc., Manitoba Masonry Institute, and Tower Engineering Group are also appreciated. Special thanks are extended to the technical staff of the W. R. McQuade Structures Laboratory at the University of Manitoba for their valuable assistance during the experimental work.

References

1. CSA (Canadian Standards Association) Group. 2024. *Design of Concrete Structures*. CSA A23.3:24. Toronto, ON, Canada: CSA Group.

2. ACI (American Concrete Institute). 2025. *Building Code for Structural Concrete—Code Requirments and Commentary (ACI CODE-318-25)*. Farmington Hills, MI: ACI.

3. Hernandez Brito, S., K. Mahmoud, K. Truderung, and E. El-Salakawy. 2022. "Behavior of Reinforcing Bar Connections of Hollow-Core Slabs to Masonry Walls under In-Plane Forces." *PCI Journal* 67 (6): 51–68. https://doi.org/10.15554/pcij67.6-03.

4. CPCI (Canadian Precast/Prestressed Concrete Institute). 2017. *CPCI Design Manual: Precast and Prestressed Concrete*. Ottawa, ON, Canada: CPCI.

5. CSA Group. 2014. *Mortar and Grout for Unit Masonry*. CSA A179-14 (R2024). Toronto, ON, Canada: CSA Group.

6. ASTM Subcommittee C15.30. 2023. *Standard Specification for Grout for Masonry*. ASTM C476-23. West Conshohocken, PA: ASTM International.

7. ASTM Subcommittee C01.27. 2024. *Standard Test Method for Compressive Strength of Hydraulic Cement Mortars (Using 50 mm [2 in.] Cube Specimens)*. ASTM C109/C109M-23. West Conshohocken, PA: ASTM International.

8. ASTM Subcommittee C15.30. 2024. *Standard Specification for Mortar for Unit Masonry*. ASTM C270-24. West Conshohocken, PA: ASTM International.

9. ASTM Subcommittee A01.13. 2024. *Standard Test Methods and Definitions for Mechanical Testing of Steel Products*. ASTM A370-24a. West Conshohocken, PA: ASTM International.

About the authors

Yazan Al-Hatamleh is a master of science student in the department of civil engineering at the University of Manitoba in Winnipeg, MB, Canada.

Yasser M. Selmy, PhD, is a lecturer in the civil engineering department at Suez Canal University in Ismailia, Egypt. He was a postdoctoral fellow in the department of civil engineering at the University of Manitoba.

Karl Truderung, MS, PEng, is a structural engineer and associate at Tower Engineering Group in Winnipeg.

Ehab F. El-Salakawy, PhD, PEng, is a professor in the department of civil engineering at the University of Manitoba. He served as the Canada Research Chair in Durability and Modernization of Civil Structures from 2006 to 2016.

Abstract

This study investigates the in-plane tensile performance of end-bearing bar connections between hollow-core slabs and concrete masonry walls, a critical component in precast concrete diaphragm systems for mid- and high-rise construction. Six full-scale wall-slab assemblies were tested under displacement-controlled pull-away loading to simulate diaphragm tension with variations in reinforcement geometry (L-shaped and U-shaped bars), parapet presence, and axial compression to reflect different floor levels. The results highlight that the primary load-resisting mechanism was shear friction at the grout-to-masonry interface, with embedded reinforcement and axial load serving to delay grout cracking and maintain structural integrity postpeak. U-bar configurations showed improved strain distribution and reduced displacement, while vertical wall reinforcement, common in western Canada practice, proved critical in confining the grout and maintaining a continuous load path. Axial compression significantly enhanced connection strength and ductility, with peak capacities reaching up to 90 kN (20 kip), well above code-prescribed minimums in the Canadian Standards Association's CSA A23.3:24, *Design of Concrete Structures*, and the American Concrete Institute's *Building Code for Structural Concrete—Code Requirements and Commentary (ACI 318-25)*. Despite severe interface cracking, all connections sustained residual tensile capacity, demonstrating the resilience of end-bearing bar connections when combined with appropriate reinforcement detailing. The findings support current design practices and offer insight into enhancing the safety and robustness of diaphragm-to-wall connections in precast concrete systems.

Keywords

Capacity, end-bearing connection, hollow-core slab, in-plane force, masonry wall, slab, western Canada.

Review policy

This paper was reviewed in accordance with the Precast/Prestressed Concrete Institute's peer-review process. The Precast/Prestressed Concrete Institute is not responsible for statements made by authors of papers in *PCI Journal*. No payment is offered.

Publishing details

This paper appears in *PCI Journal* (ISSN 0887-9672) V. 71, No. 4, July–August 2026, and can be found at https://doi.org/10.15554/pcij71.4-01. *PCI Journal* is published bimonthly by the Precast/Prestressed Concrete Institute, 8770 W. Bryn Mawr Ave., Suite 1150, Chicago, IL 60631.

Reader comments

Please address any reader comments to *PCI Journal* journal@pci.org or Precast/Prestressed Concrete Institute, c/o *PCI Journal*, 8770 W. Bryn Mawr Ave., Suite 1150, Chicago, IL 60631.